Plant Soil (2020) 454:343–358
https://doi.org/10.1007/s11104-020-04656-4

REGULAR ARTICLE

Phytolith-rich straw application and groundwater table management over 36 years affect the soil-plant silicon cycle of a paddy field

Xiaomin Yang · Zhaoliang Song · Zhilian Qin · Lele Wu · Lichu Yin · Lukas Van Zwieten · Alin Song · Xiangbin Ran · Changxun Yu · Hailong Wang

Received: 14 May 2020 / Accepted: 28 July 2020 / Published online: 6 August 2020

Abstract

Background and aims Silicon (Si) deficiency is a major constraint on rice production. The objective of this study was to evaluate the long-term influence of phytolith-rich straw return and groundwater table management on labile Si fractions in paddy soil and subsequent plant Si uptake.

Methods A field experiment was conducted over 36 years in subtropical China with different application doses of phytolith-rich straw and a groundwater table of either 20 or 80 cm. An optimized sequential chemical extraction procedure allowed us to determine labile Si fractions, represented by $CaCl_2$-Si, Acetic-Si, H_2O_2-Si, Oxalate-Si, and Na_2CO_3-Si. Additional analyses included the determination of amorphous silica particles in soil, phytoliths in supplied straw, Si in planted rice straw, and the dissolution rate of phytoliths extracted from supplied straw.

Results Long-term application of phytolith-rich straw significantly increased the H_2O_2-Si and Na_2CO_3-Si

Responsible Editor: Miroslav Nikolic

X. Yang · Z. Song (✉) · L. Wu
Institute of Surface-Earth System Science, School of Earth System Science, Tianjin University, Tianjin 300072, China
e-mail: zhaoliang.song@tju.edu.cn

Z. Qin
Faculty of Resource and Environment Sciences, Hunan Normal University, 410081 Changsha, China

L. Yin
College of Resources and Environment, Hunan Agricultural University, 410128 Changsha, China

L. Van Zwieten
New South Wales Department of Primary Industries, 1243 Bruxner Highway, Wollongbar, NSW 2477, Australia

A. Song
Key Laboratory of Crop Nutrition and Fertilization, Institute of Agricultural Resources and Regional Planning, Chinese Academy of Agricultural Sciences, 100081 Beijing, China

X. Ran
First Institute of Oceanography, Ministry of Natural Resources, No. 6 Xianxialing Road, 266061 Qingdao, China

C. Yu
Department of Biology and Environmental Science, Linnaeus University, 39182 Kalmar, Sweden

H. Wang
School of Environmental and Chemical Engineering, Foshan University, 528000 Foshan, Guangdong, China

H. Wang
Key Laboratory of Soil Contamination Bioremediation of Zhejiang Province, Zhejiang A&F University, Hangzhou, Zhejiang 311300, China

contents. The $CaCl_2$-Si (5.21–7.91 mg kg^{-1}), H_2O_2-Si (50.0–72.4 mg kg^{-1}) and Na_2CO_3-Si (3.33–4.60 g kg^{-1}) contents were positively correlated with soil organic carbon. The Si content (13.6–28.9 g kg^{-1}) in planted rice straw significantly ($p < 0.05$) increased with the application dose of phytolith-rich straw under both groundwater tables. This effect was significantly ($p < 0.05$) greater under 80 cm groundwater table than under 20 cm groundwater table for matching straw amendments.

Conclusions This study indicates that long-term application of phytolith-rich straw and groundwater management significantly increase soil Si bioavailability by promoting accumulation of organic matter and phytoliths, and enhancing the soil-plant Si cycle.

Keywords Straw return · Hydragric Anthrosols · Rice · Phytolith · Silicon bioavailability · Subtropical China

Introduction

Silicon (Si) is the second most abundant element in the Earth's crust and is beneficial for higher plants, especially monocotyledons (Takahashi et al. 1990; Epstein 1999; Ma and Yamaji 2006). As one of the most important cereal crops across the globe, rice (*Oryza sativa* L.) is a typical Si-accumulating plant (Epstein 1999; Li et al. 2013; Guo et al. 2015). Silicon is deposited as amorphous silica forming phytoliths in the cell wall, cell lumen and intercellular spaces, and as Si-double layers beneath the cuticle after plant absorption of the dissolved Si in the form of silicic acid [$Si(OH)_4$ or H_4SiO_4] from soil solution (Epstein 1999; Ma and Yamaji 2006; Coskun et al. 2019). Generally, ~90% of silica in rice plants occurs as phytoliths (Guo et al. 2015; Song et al. 2015). As the largest rice producer in the world, China has 31 million ha of paddy fields producing around 204 million tons of rice per year (Deng et al. 2019; Wang and Hijmans 2019). According to the global average grain-straw ratio of 1.21 (Domínguez-Escribá and Porcar 2010), this would equate to the production of about 247 million dry tons of rice straw annually. Notably, more than 80% of paddy fields in China are located in subtropical regions (CFNDC 2019), and most of them are suffering from Si deficiency due to low soil pH, high soil weathering and leaching, and long-term intensive rice cultivation (Liang et al. 2015). Si deficiency in paddy fields has recently been recognized as a limiting factor for sustainable rice production (Liang et al. 2015; Klotzbücher et al. 2015; Li and Delvaux 2019).

Generally, Si as well as other nutrients (e.g. nitrogen (N), phosphorus (P), and potassium (K)) taken up by rice plants remain largely in the straw at crop maturity (Dobermann and Fairhurst 2002; Klotzbücher et al. 2015; Marxen et al. 2016). Li and Delvaux (2019) estimated that the removal of rice straw and husks from paddy fields results in an annual loss of 83.4 Tg phytogenic amorphous silica (PhSi) worldwide. Returning the phytolith-rich straw associated materials could therefore provide a way to replenishing the bioavailable Si pool in paddy fields (Keller et al. 2012; Seyfferth et al. 2013; Marxen et al. 2016; Klotzbücher et al. 2018), and has been increasingly investigated. For example, in a study in California, the incorporation of phytolith-rich rice straw has been suggested as a low-cost means to increase the bioavailable Si pool, resulting in higher Si accumulation in aboveground biomass (Seyfferth et al. 2013). It has also been shown that the recycling of phytolith-rich rice straw ash increases the bioavailable Si content in soil solution during the fallow period and thus significantly enhances Si accumulation in rice straw at the tillering stage in the first cropping season (Klotzbücher et al. 2018). These experiments demonstrate that incorporation of phytolith-rich straw residues enhances rice production (Song et al. 2014a; Memon et al. 2018), especially in highly weathered soils (Li et al. 2020a).

Apart from the recycling of phytoliths from straw, the soil-plant Si cycle can be strongly influenced by the interactions among a variety of relatively labile Si fractions, including water-soluble Si, labile Si adsorbed on the surfaces of inorganic soil particles, labile Si loosely adsorbed on the surfaces of soil organic matter, Si occluded in pedogenic oxides/hydroxides, and biogenic and pedogenic amorphous silica (Cornelis et al. 2011; White et al. 2012; Liang et al. 2015; Georgiadis et al. 2013; Li et al. 2020a; Yang et al. 2020). In general, water-soluble Si in soil solution can be adsorbed on the surfaces of various inorganic, organic and organic-inorganic colloids such as clays, soil organic matter and organic-inorganic complexes in soils (Georgiadis et al. 2013; Song et al. 2014a; Liang et al. 2015). The abundant pedogenic oxides and hydroxides in soils also play an important role in adsorption, occlusion and release of silicic acid (Cornelis et al. 2011; Georgiadis et al. 2013; Yang et al. 2020). Considering that the

dissolution rate of biogenic amorphous silica is estimated to 2–4 orders of magnitude higher than that of typical soil and rock minerals (Fraysse et al. 2006, 2009), this form of silica has thus been suggested as a major source of bioavailable Si for plant over short-time scales (e.g., White et al. 2012; Seyfferth et al. 2013; Li and Delvaux 2019).

In subtropical China, many paddy soils are commonly located in regions with highly variable groundwater depths. The fluctuation in groundwater levels can result in repeated wetting and drying cycles, which may influence the interaction between iron (Fe) or aluminum (Al) oxides/hydroxides and relatively labile Si fractions (Hodson and Sangster 1999; Pokrovski et al. 2003; Beardmore et al. 2016; Georgiadis et al. 2017). In general, adsorbed Si on the surface of Fe and Al oxides and occluded Si in these oxides will be released under reducing and acidic conditions (Siipola et al. 2016). A subsequent shift to oxidizing and neutral conditions promotes the formation of Fe and Al oxides and enables adsorption, occlusion and co-precipitation of Si on/with these oxides (Siipola et al. 2016). In addition, Jones and Handreck (1963) emphasized that Al oxides had a greater effect than Fe oxides on the solubility of silica in soil solution. A field experiment under different water regimes showed that water conservation irrigation can change the seasonal variation of Si concentration in the soil solution, but its effects on the Si uptake by rice is insignificant (Mihara et al. 2016). Considering the experiment conducted by Mihara et al. (2016) was over a duration of only three years, a paucity of information remains on the longer-term role of different water regimes on soil Si bioavailability and the soil-plant Si cycle.

Although studies have focused on the impact of phytolith-rich straw residues on the soil bioavailable Si (e.g., Guntzer et al. 2012; Song et al. 2014a; Marxen et al. 2016), the interactions amongst the labile Si pools under different water regimes are rarely considered, and data have not been considered in terms of long-term biogeochemical process. To address these significant gaps in knowledge, this study used a 36-year field experiment involving growing rice in subtropical China to evaluate the long-term effect of phytolith-rich straw application and groundwater management on the soil-plant Si cycle. It was hypothesized that: (i) long-term phytolith-rich straw application would significantly increase organic carbon storage and the amorphous Si pool in soil; (ii) the soil-plant Si cycle in paddy fields would be influenced by the long-term phytolith-rich straw application; and (iii) soil Si bioavailability and the transformation of different labile Si fractions would be influenced by groundwater height.

Materials and methods

Study site and experimental design

The study site was located on the experimental farm of Hunan Agricultural University in Changsha, Hunan Province, China (28°18′ N, 113°08′ E). This area has a subtropical monsoon climate with a mean annual precipitation of 1362 mm and a mean annual temperature of 17.2 (Yin et al. 2015). The altitude of the study site is 50 m above sea level. Paddy soils, which are equivalent to hydragric anthrosols based on the Food and Agriculture Organization (FAO) soil classification system (IUSS Working Group WRB 2015), are widely distributed in this area. Early rice (*Oryza sativa* L.)-late rice-winter fallow is a typical rotation system in this area.

A long-term experiment consisting of 36 plots with early rice-late rice-winter fallow rotation was established in 1982 (Yin et al. 2015). Three straw application treatments were evaluated, including: CF, application of only N, P, and K fertilizers (urea, calcium superphosphate, potassium chloride); LOM, application of a small amount of straw supplying one-third of the total fertilizer N; HOM, application of a large amount of straw supplying two-third of the total fertilizer N. Each treatment had 2 water table depths (20 and 80 cm). There were 3, 6 and 3 replicates for the CF, LOM and HOM treatments, respectively under both groundwater tables (Fig. 1). For the CF treatment, the rates of applied chemical fertilizers were 150 kg N, 75 kg P_2O_5, and 150 kg K_2O per ha in both the early and late rice seasons (Yin et al. 2015). The applied straw material was rice straw before 2012, while it was changed to maize straw after 2012 (Lin et al. 2018). Notwithstanding, both rice straw and maize straw are phytolith-rich straw materials (Song et al. 2014b). The average contents of N, P, and K in supplied rice straw were 5.03, 1.82, and 13.2 g kg^{-1}, respectively (Yin et al. 2015); and the average contents of N, P, and K in supplied maize straw were 10.4, 5.93, and 12.6 g kg^{-1}, respectively (Lin et al. 2018). Thus, the average application rates of rice straw in LOM and HOM treatments were approximately 20 and 40 t ha^{-1} $year^{-1}$, respectively. The average application rates of

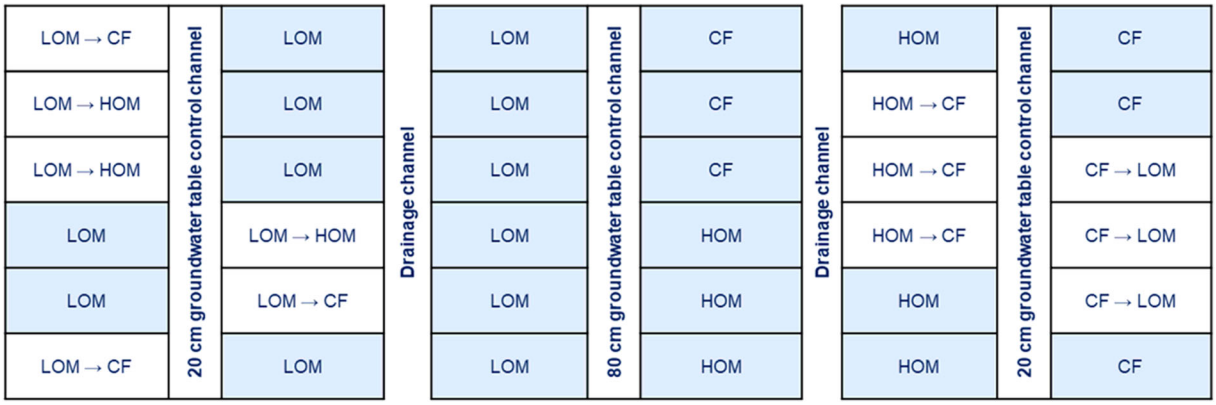

Fig. 1 Schematic illustration of the 36 long-term experimental plots (modified from Yin et al. 2015). This study only focused on the CF, LOM, and HOM treatments under 20 and 80 cm groundwater tables; the white plots (i.e., LOM→CF, LOM→HOM, HOM→CF, and CF→LOM treatments) were not considered in this study

maize straw in LOM and HOM treatments were approximately 10 and 20 t ha^{-1} $year^{-1}$, respectively. To ensure uniform inputs of P and K in all treatments, chemical fertilizers (calcium superphosphate and potassium chloride) were used to supplement the P and K deficiencies in the LOM and HOM treatments.

All chemical fertilizers and supplied phytolith-rich straw were mixed and applied to the tillage layer of each plot annually during the fallow period. The supplied phytolith-rich straw was crushed (< 10 mm) before being returned to soil. In each plot, 35 plants of the early rice cultivar (Xiangzaoxian) were planted in April and harvested in July. Thirty-five plants of the late rice cultivar (VY46) were then planted in each plot and harvested in October. The soils were flooded from March to October (i.e., the rice-growing season) and drained from November to February (i.e., the fallow season) each year.

Sample collection and treatment

A cutting ring (100 cm^3) was used to collect soil samples (0–20 cm) for this study in October 2018. The soil sample from each plot was thoroughly air-dried, weighed, ground, and then passed through 10 mesh (2 mm) followed by 100 mesh (0.15 mm pore size) sieves. The straw from two clumps of rice plants in each plot was also collected and mixed thoroughly into a composite sample for each plot. The straw samples were washed with distilled water, dried to constant weight at 65 , weighed, mixed, and then divided into two subsamples. One of the sub-samples was crushed into powder, and the another was cut into small pieces (< 5 mm).

Basic soil analyses

Soil bulk density (BD) was determined using the cutting-ring method (Lu 2000). Particle size analysis of the soils (10 mesh) was completed using a laser particle size analyzer (Mastersizer 3000, Malvern, UK). The pH (soil : water = 1 : 2.5 w/w) and electrical conductivity (EC) (soil : water = 1 : 5 w/w) of the 10 mesh soil samples were measured using a pH/conductivity meter (Star A215, Thermo Scientific, USA) (Lu 2000). Approximately 0.1 g of soil sample (100 mesh) was used to determine the soil organic carbon (SOC) content using the Walkley and Black method (Lu 2000; Walkley and Black 1934).

Extraction of different labile Si fractions in soil

Five sub-fractions of labile Si (as listed below) were defined and extracted by an optimized sequential chemical extraction process. The content of the total labile Si was the sum of the five sub-fractions.

i) *Easily soluble Si* ($CaCl_2$-Si): A total of 2 g of soil sample (10 mesh) was slowly shaken (linearly) for 16 h with 20 mL 0.01 M $CaCl_2$ (i.e., soil : solution = 1 : 10 w/v) in a 50 mL polypropylene centrifuge tube at 25 (Haysom and Chapman 1975; Sauer et al. 2006). After extraction, the samples were centrifuged at 1760 × g for 5 min, and the supernatant was filtered through a 0.45 μm cellulose acetate filter in order to remove the possible interference of suspended particles. This extract was prepared for analysis of $CaCl_2$-Si.

ii) *Labile Si adsorbed on the surfaces of inorganic soil particles* (Acetic-Si): The soil residue from step (i) was washed with deionized water and dried at 65 . Once dry, 20 mL of 0.01 M acetic acid was added (i.e., soil : solution = 1 : 10 w/v) and then shaken (linearly) for 24 h at 25 (Georgiadis et al. 2013). The shaken samples were centrifuged and filtered as described in step i). The extract was prepared for analysis of Acetic-Si.

iii) *Labile Si loosely adsorbed on the surfaces of soil organic matter* (H_2O_2-Si): After the soil residue from step (ii) was washed with deionized water, 10 mL of H_2O_2 (AR, 30%) was slowly added (Georgiadis et al. 2013; Song et al. 2014a). When the initial reaction at room temperature was complete (i.e., no longer fizzing), the centrifuge tube containing samples was put into a water bath at 85 until the reaction was again complete. The sample was then dried at 65 in a ventilation oven. Once dry, the samples were mixed with 20 mL of 1 m Na-acetate buffer solution (pH = 4.0), and then slowly shaken (linearly) for 24 h at 25 . The shaken samples were centrifuged and filtered as described in step i). The extract was prepared for analysis of H_2O_2-Si. It should be noted that hot H_2O_2 solution also leads to a partial release of Si from poorly crystalline as well as crystalline silicates (e.g., kaolin, microcline, quartz) (Georgiadis et al. 2013). Thus, the labile Si loosely adsorbed on the surfaces of soil organic matter extracted by H_2O_2 might be overestimated. As there is no better method for extraction of this Si fraction at present, H_2O_2-extraction was still recommended by Georgiadis et al. (2013) and included in their sequential extraction experiment.

iv) *Occluded Si in poorly aluminosilicates and weakly ordered sesquioxides* (Oxalate-Si): The soil residue from step (iii) was washed with deionized water and then dried at 65 in a ventilation oven. Once dry, 40 mL of 0.2 M NH_4-oxalate buffer solution (pH = 3.0) was added to 0.8 g of the dried sample (i.e. soil : solution = 1 : 50 w/v) in a 50 ml polypropylene centrifuge tube and slowly shaken for 1 h in a dark room (Saccone et al. 2007; Cornelis et al. 2011; Barão et al. 2014). The shaken samples were centrifuged and filtered as described in step i). The extract was prepared for the analysis of Oxalate-Si.

v) *Amorphous Si* (Na_2CO_3-Si): The Na_2CO_3 protocol proposed by DeMaster (1981) was widely used to determine soil amorphous Si content. It should be noted that this protocol may not be efficient to dissolve aged phytoliths (Meunier et al. 2014). As the aged phytoliths were rare in our studied soils, the Na_2CO_3-extraction was also used to determine soil amorphous Si in this study. The soil residue from step (iv) was washed with deionized water and then dried at 65 °C in a ventilation oven. Once dry, 40 mL of 1% Na_2CO_3 solution (pH = 11.2) was added to 30 mg of the dried sample in a 50 mL polypropylene centrifuge tube and digested in a shaker bath at 85 °C for 6 h with the cap slightly loosened to vent gas. After 1 h, the dissolution was stopped by cooling the sample in a cold-water bath. A 1 mL aliquot was sampled and neutralized with 9 mL of 0.021 M HCl. Digestion was restarted in the bath at 85 and the sub-sampling procedure repeated a further five times (i.e., after 2, 3, 4, 5, and 6 h digestion). The amounts of extracted Si were plotted versus time. The first part of the curve, for sampling at 1 and 2 h, represented the rapid dissolution of amorphous silica particles (DeMaster 1981; Cornelis et al. 2011; Meunier et al. 2014). The second linear part, calculated using sampling at 3, 4, 5, and 6 h, corresponded to the slower dissolution of crystalline silicates (DeMaster 1981; Cornelis et al. 2011; Meunier et al. 2014). The intercept of the linear phase at $t = 0$ was regarded as the percentage of Na_2CO_3-Si (DeMaster 1981; Cornelis et al. 2011; Meunier et al. 2014).

Determination of total Si and stable Si

To determine the total Si content in soils and plants, ~ 30 mg soil samples (100 mesh) and ~ 50 mg plant samples (powder) were fused with Li-metaborate (~ 300 mg) at 950 for 30 min, respectively. The obtained "fusion cake" was dissolved with 30 mL dilute nitric acid (4%). The Si concentrations in all the above extracts were determined using the molybdenum blue colorimetric method (Lu 2000) with an ultraviolet-visible spectrophotometer (UV-1800, Shimadzu, Japan). Quality assurance for the analysis of Si was monitored using a standard soil sample (GBW07405) and a precision of 7% was obtained. The soil stable Si fraction was estimated as the difference between the soil total Si and the sum of all labile Si fractions (Georgiadis et al. 2013, 2017).

Extraction of amorphous silica particles from soils and plants

Approximately 2 g of supplied dry rice straw (6 replicates) and maize straw (9 replicates) were used to extract amorphous silica particles (i.e., phytoliths) using a wet digestion method as described by Parr and Sullivan (2014). A wet oxidation and heavy liquid suspension ($ZnBr_2$, $\rho = 2.3$ g cm^{-3}) method (Zuo et al. 2014) was used to isolate amorphous silica particles from 10 g soil samples in each plot. The extracted amorphous silica particles from plants and soils were cleaned up using the Walkley-Black method (Walkley and Black, 1934) to ensure that all extraneous organic materials other than the amorphous silica particles were thoroughly removed (Li et al. 2013). These amorphous silica particles were then oven-dried at 65 °C for 24 h in a centrifuge tube and weighed to obtain the content after cooling. The purification and composition of amorphous silica particles extracted from soils was identified using a light microscope (BX53, Olympus, Japan) with 200 × and 400 × magnification, respectively.

Determination of fresh phytolith dissolution

The Si contents in extracted phytoliths from supplied rice straw and maize straw were determined using the same methods as determination of total Si in soils and plants. A sequence of solutions (pH = 1, 2, 3, 4, 5, 5.5, 6, 6.5, 7, 8, 9, 9.5, 10, 10.5, 11, 12) were prepared with hydrochloric acid, sodium hydroxide, and deionized water. Approximately 10 mg of phytoliths (3 replicates) from the supplied phytolith-rich straw materials (i.e., rice straw and maize straw) were added to 50 mL of each of the 16 solutions with different pH values in 50 mL polypropylene tubes. These solutions were kept at room temperature. The Si concentrations in those solutions were determined at both 15 and 60 days using the molybdenum blue colorimetric method as previously described. The phytolith dissolution rate was calculated as follows:

$$PDR_{15} = \frac{V \times Si_{15}}{W_{phytolith} \times Si_{phytolith}} \times 100\% \quad (1)$$

$$PDR_{60} = \frac{(V - V_{15}) \times Si_{60}}{W_{phytolith} \times Si_{phytolith} - V_{15} \times Si_{15}} \times 100\% \quad (2)$$

where PDR_{15} and PDR_{60} is the phytolith dissolution rate (%) after 15 days and 60 days, respectively; V is the original volume of solution (mL) used to dissolved phytoliths (i.e., 50 mL); V_{15} and V_{60} is the volume of solution (mL) sampled to determine Si concentration after 15 days and 60 days, respectively; Si_{15} and Si_{60} is the Si concentration (μg mL^{-1}) in remaining solution after 15 days and 60 days, respectively; $W_{phytolith}$ is the weight of phytoliths (mg) used for the dissolution experiment; $Si_{phytolith}$ is the Si content (g kg^{-1}) in supplied phytoliths.

To evaluate the effect of contamination from any residual organic matter on phytolith dissolution, the carbon contents in the extracted phytoliths were also determined. The results showed that the carbon contents in phytoliths extracted from supplied rice straw and maize straw were lower than 5 g kg^{-1} (unpublished data). As phytoliths generally occlude some carbon (1 ~ 60 g kg^{-1}) during their formation (Li et al. 2013; Song et al. 2014b, 2015; Zuo et al. 2014; Guo et al. 2015), our determined C (< 5 g kg^{-1}) was mainly of phytolith-occluded carbon. This could, therefore, verify the lack of contamination by organic residue.

Statistical analyses

The Shapiro-Wilk test was used to evaluate the normality of distribution of the data (SPSS 18.0). Pearson correlation and partial correlation coefficients were analyzed using Excel 2016 and SPSS 18.0. Independent sample *t*-test and one-way analysis of variance (ANOVA) with the least significant difference (LSD) test were performed to examine the differences between data groups (SPSS 18.0).

Results

Soil physiochemical properties

The highest soil bulk density (BD) was found in the CF treatment for the 20 cm (1.24 ± 0.07 g cm^{-3}) and 80 cm (1.39 ± 0.07 g cm^{-3}) groundwater tables (Table 1). The volume percentage of soil clay (< 2 μm) ranged from 14.3 ± 0.91% to 16.6 ± 0.02%, silt (2–50 μm) ranged from 78.2 ± 1.23% to 82.0 ± 1.91%, fine sand (50–250 μm) ranged from 2.60 ± 0.20% to 3.08 ± 0.15%, and coarse sand (> 250 μm) ranged from 0.61 ± 0.50% to 1.90 ± 0.68% (Table 1). The pH of CF was higher

Table 1 Soil physicochemical properties under different treatments. Data are presented as the means ± standard deviations

Water table	Treatment	BD ($g\ cm^{-3}$)	Particle size (%)				pH	EC ($\mu s\ cm^{-1}$)	SOC ($g\ kg^{-1}$)
			Clay (< 2 μm)	Silt (2–50 μm)	Fine sand (50–250 μm)	Coarse sand (> 250 μm)			
20 cm	CF	1.24 ± 0.07Aa	16.6 ± 0.02Aa	78.6 ± 1.09Bb	2.84 ± 0.49Aa	1.90 ± 0.68Aa	5.19 ± 0.07Aa	83.7 ± 9.04Aa	13.1 ± 1.69Ac
	LOM	1.12 ± 0.07Bb	14.9 ± 1.64Aa	81.8 ± 1.76Aa	2.72 ± 0.64Aa	0.63 ± 0.40Ab	4.90 ± 0.07Bb	100 ± 19.5Aa	18.6 ± 0.70Ab
	HOM	1.02 ± 0.06Ab	16.7 ± 0.51Aa	78.2 ± 1.23Bb	3.08 ± 0.15Aa	2.02 ± 1.10Aa	4.84 ± 0.02Bb	95.4 ± 14.2Aa	23.0 ± 1.52Aa
80 cm	CF	1.39 ± 0.09Aa	15.5 ± 0.30Ba	80.6 ± 0.51Aa	3.06 ± 0.52Aa	0.84 ± 0.26Aa	5.45 ± 0.13Aa	48.2 ± 0.94Bb	12.7 ± 0.54Ac
	LOM	1.23 ± 0.06Ab	14.9 ± 1.22Aa	81.4 ± 2.64Aa	3.06 ± 1.41Aa	0.61 ± 0.50Aa	5.11 ± 0.07Ab	57.7 ± 4.12Ba	17.3 ± 0.51Bb
	HOM	1.10 ± 0.03Ac	14.3 ± 0.91Ba	82.0 ± 1.91Aa	2.60 ± 0.20Ba	1.08 ± 0.77Aa	5.05 ± 0.02Ab	52.6 ± 4.23Bab	19.7 ± 0.59Ba

Different upper-case letters in a column indicate significant differences of the same treatment under different groundwater tables at $p < 0.05$, based on the independent sample *t*-test. Different lower-case letters in a column indicate significant differences among treatments under the same groundwater table at $p < 0.05$, based on the least significant difference (LSD) test

than that of the LOM and HOM treatments for both the 20 cm and the 80 cm groundwater tables (Table 1). The EC in all treatments with the 20 cm groundwater table was higher than in all treatments with the 80 cm groundwater table (Table 1). The SOC content in the CF treatment was 13.1 ± 1.69 g kg^{-1}, which increased significantly ($p < 0.05$) to 18.6 ± 0.70 g kg^{-1} in the LOM treatment, with a further significant increase to 23.0 ± 1.52 g kg^{-1} in the HOM treatment for the 20 cm groundwater table (Table 1). Under the 80 cm groundwater table, the highest SOC content was found in the HOM treatment (19.7 ± 0.59 g kg^{-1}) followed by the LOM treatment (17.3 ± 0.51 g kg^{-1}) and the CF treatment (12.7 ± 0.54 g kg^{-1}) (Table 1). Except for the CF treatment, the SOC content in both the LOM and HOM treatments under the 20 cm groundwater table was significantly higher than that in the equivalent treatments under the 80 cm groundwater table (Table 1). Pearson correlation analysis showed a negative correlation ($p < 0.01$) between SOC and soil pH at both groundwater depths (Fig. 2).

Si fractions

The total Si content in soil ranged from 280 ± 12.7 g kg^{-1} to 297 ± 9.27 g kg^{-1} and was found mainly as the stable Si fraction (276–293 g kg^{-1}), with no significant differences between treatments or groundwater depths (Table 2). The labile Si fraction varied from 3.60 ± 0.29 g kg^{-1} to 4.86 ± 0.42 g kg^{-1} and increased ($p < 0.05$) with increasing phytolith-rich straw application at both groundwater depths, whereas there were no differences between equivalent treatments under different groundwater depths (Table 2). Within the labile Si fractions, the largest contributor was Na_2CO_3-Si (3.33–4.60 g kg^{-1}), followed by Oxalate-Si (125–208 mg kg^{-1}), H_2O_2-Si (50.0–71.8 mg kg^{-1}), Acetic-Si (13.8–16.1 mg kg^{-1}), and $CaCl_2$-Si (5.21–7.91 mg kg^{-1}) (Table 2). The $CaCl_2$-Si contents for the LOM and HOM treatments under the 80 cm groundwater table were significantly higher than under the 20 cm groundwater table (Table 2). The contents of the H_2O_2-Si and Na_2CO_3-Si fractions increased with the increasing amount of phytolith-rich straw application under both groundwater depths (Table 2).

The SOC content was positively correlated (Pearson correlation) with $CaCl_2$-Si, H_2O_2-Si and Na_2CO_3-Si contents under both groundwater depths (Table 3). According to the Pearson correlation analysis, pH was

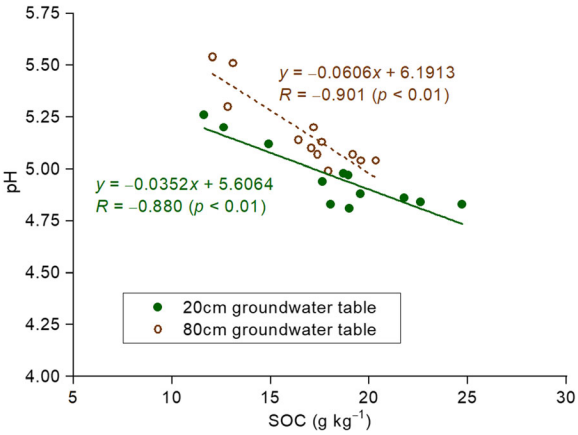

Fig. 2 Pearson correlations between SOC and soil pH in each plot under 20 and 80 cm groundwater tables

correlated negatively with $CaCl_2$-Si, H_2O_2-Si, and Na_2CO_3-Si under the 80 cm groundwater table (Table 3), but only H_2O_2-Si and Na_2CO_3-Si contents showed a significant negative correlation with soil pH under the 20 cm groundwater table (Table 3). Partial correlation analysis showed that the SOC content was also correlated positively with the $CaCl_2$-Si, H_2O_2-Si, and Na_2CO_3-Si contents under the 20 cm groundwater table, but only correlated positively with $CaCl_2$-Si and H_2O_2-Si contents under the 80 cm groundwater table (Table 3). According to partial correlation analysis, soil pH did not show any correlation with the various labile Si fractions (Table 3).

Under the two groundwater tables, Pearson correlation analysis showed that Na_2CO_3-Si content was positively correlated with H_2O_2-Si and $CaCl_2$-Si, and there was also a positive correlation between H_2O_2-Si and $CaCl_2$-Si (Fig. 3). Partial correlation analysis showed that the Acetic-Si content had a positive correlation with Na_2CO_3-Si and H_2O_2-Si under the 20 cm groundwater tables, whereas H_2O_2-Si was positively correlated with Na_2CO_3-Si and $CaCl_2$-Si under the 80 cm groundwater table (Fig. 3).

Amorphous silica particle content in soils and supplied straw materials

The content of soil amorphous silica particles significantly increased with increasing rates of phytolith-rich straw application under both groundwater regimes (Fig. 4). These particles were mainly composed of phytoliths and involved a small number of diatoms and diatom frustules as observed by microscopy (Fig. 5). The content of soil amorphous silica particles with CF treatment under the 20 cm groundwater table was 4.09 ± 0.17 g kg^{-1}, that for LOM treatment was higher ($p < 0.05$) at 4.82 ± 0.39 g kg^{-1}, and that for HOM treatment was the highest ($p < 0.05$) at 6.36 ± 0.23 g kg^{-1} (Fig. 4). Under the 80 cm groundwater table, CF treatment gave 4.48 ± 0.34 g kg^{-1}, LOM treatment 5.49 ± 0.56 g kg^{-1}, and HOM treatment 6.93 ± 0.75 g kg^{-1}; each of these values being significantly ($p < 0.05$) different (Fig. 4). Additionally, the content of plant amorphous silica particles (i.e., phytoliths) in supplied rice straw and maize straw was 67.6 ± 20.2 g kg^{-1} and 21.9 ± 1.2 g kg^{-1}, respectively (Fig. 6a).

Phytolith dissolution rate

The Si content in phytoliths extracted from supplied rice straw and maize straw was 436 ± 12.3 g kg^{-1} and 426 ± 17.8 g kg^{-1}, respectively (Fig. 6a). The dissolution rates (Eqs. 1 and 2) of phytoliths from rice and maize straw that were used in the field trials increased slightly as the pH increased from 2.0 to 5.5 (in solution) (Fig. 6b). When the pH was greater than 5.5, the dissolution rates of the these phytoliths increased exponentially (Fig. 6b). Our results also showed that the dissolution rates of supplied rice straw phytoliths were generally higher than those of maize straw phytoliths (Fig. 6b). Under the pH experienced under field conditions (i.e., pH ≤ 5.5), only 0.20–0.56% of maize straw phytoliths and 0.27–0.79% of rice straw phytoliths dissolved after 15 days. Over 60 days, 0.62–1.53% of the maize straw phytoliths dissolved, compared to 0.92–2.03% for the rice straw.

Si contents in planted rice straw

The Si content in planted rice straw ranged from 13.6 ± 2.26 g kg^{-1} to 21.3 ± 0.55 g kg^{-1} under the 20 cm groundwater table and from 18.4 ± 1.69 g kg^{-1} to 28.9 ± 5.50 g kg^{-1} under the 80 cm groundwater table (Fig. 7). The Si contents in planted rice straw increased significantly ($p < 0.05$) with increasing rate of phytolith-rich straw application under both groundwater depths. The highest Si content in planted rice straw was found with the HOM treatment and the lowest with the CF treatment irrespective of groundwater height. In all treatments, the Si contents in planted rice straw under the 20 cm groundwater table were significantly ($p < 0.05$) lower than those under the 80 cm groundwater table.

Table 2 Content of each Si fraction under different treatments. Data are presented as means ± standard deviation

Water table	Treatment	Total Si (g kg^{-1})	Labile Si						Stable Si (g kg^{-1})
			$CaCl_2$-Si (mg kg^{-1})	Acetic-Si (mg kg^{-1})	H_2O_2-Si (mg kg^{-1})	Oxalate-Si (mg kg^{-1})	Na_2CO_3-Si (g kg^{-1})	Total (g kg^{-1})	
20 cm	CF	297 ± 9.27Aa	5.21 ± 1.33Aa	14.7 ± 0.39Aab	54.7 ± 4.15Ac	208 ± 39.8Aa	3.33 ± 0.26Ac	3.60 ± 0.29Ac	293 ± 9.51Aa
	LOM	280 ± 12.7Aa	5.72 ± 0.62Ba	13.8 ± 0.63Bb	62.3 ± 2.47Ab	135 ± 22.9Ab	3.90 ± 0.19Ab	4.11 ± 0.18Ab	276 ± 12.8Aa
	HOM	297 ± 2.17Aa	6.70 ± 0.66Ba	15.0 ± 0.96Aa	72.4 ± 7.52Aa	190 ± 38.5Aa	4.56 ± 0.30Aa	4.82 ± 0.29Aa	292 ± 2.18Aa
80 cm	CF	292 ± 0.69Aa	6.78 ± 0.41Aa	16.1 ± 1.29Aa	50.0 ± 1.15Ac	185 ± 0.56Aa	3.47 ± 0.21Ac	3.71 ± 0.21Ac	289 ± 0.86Aa
	LOM	293 ± 11.8Aa	7.78 ± 0.56Aa	15.6 ± 0.78Aa	63.8 ± 2.30Ab	125 ± 20.2Ab	3.98 ± 0.19Ab	4.17 ± 0.18Ab	290 ± 11.8Aa
	HOM	297 ± 1.11Aa	7.91 ± 1.52Aa	15.9 ± 0.67Aa	71.8 ± 6.37Aa	189 ± 33.0Aa	4.60 ± 0.43Aa	4.86 ± 0.42Aa	293 ± 10.8Aa

Different upper-case letters in a column indicate significant differences of the same treatment under different groundwater tables at $p < 0.05$, based on the independent sample t-test. Different lower-case letters in a column indicate significant differences among treatments under the same groundwater table at $p < 0.05$, based on the least significant difference (LSD) test

Discussion

Effect of long-term straw application on the soil-plant Si cycle

The results of this study support previous findings (Yin et al. 2015) that long-term incorporation of crop straw into soil, in this case over a 36-year period, increased SOC accumulation (Table 1). In addition, a negative correlation was observed between SOC content and soil pH (Fig. 2). A large amount of amino acid and humic acid produced from the decomposition of straw (Cao et al. 2019) is likely to contribute to this. The rhizodeposition of rice plants and the products from microbial metabolism have also been shown to contribute to organic acid content in paddy soil (Strobel 2001; Jones et al. 2003) with flooded conditions favoring the accumulation of these organic acids (Gotoh and Onikura 1971).

Quantitative analyses of different labile Si fractions in soil is a prerequisite to understanding the soil-plant Si cycle (Georgiadis et al. 2017; Yang et al. 2020), but the contents of the various labile Si fractions are likely to be significantly influenced by changes in SOC and pH (Fraysse et al. 2009; Meunier et al. 2018; Li et al. 2019; Yang et al. 2020). For example, the $CaCl_2$-Si in sugar production soils from South Africa (Miles et al. 2014) and in rice production soils from South India (Meunier et al. 2018) were positively correlated with soil pH. However, the Pearson correlation between $CaCl_2$-Si and soil pH was negative in our study (Table 3). The SOC content was, however, significantly positively correlated with soil pH (Fig. 2), contrasting with results presented by Miles et al. (2014) and Meunier et al. (2018). Therefore, the negative correlation between $CaCl_2$-Si and soil pH in this study is likely caused by the autocorrelation effect between SOC and soil pH. To remove the autocorrelation effects between SOC and soil pH (Fig. 2), a partial correlation analysis was used to measure the statistical dependencies between SOC (or soil pH) and the various labile Si fractions. The partial correlation analysis showed that the contents of the Na_2CO_3-Si, H_2O_2-Si, and $CaCl_2$-Si fractions under the two groundwater tables were non-significantly correlated with soil pH, but they were significantly correlated with SOC content, excepting for Na_2CO_3-Si under the 80 cm groundwater table (Table 3). As a proxy of soil organic matter, the changes in SOC were mainly caused by the different doses of

Table 3 Pearson correlation coefficients and partial correlation coefficients between the various labile Si fractions and SOC, and between the various labile Si fractions and soil pH under 20 and 80 cm groundwater tables

Labile Si fractions	SOC				pH			
	Pearson correlation coefficient (pH uncontrolled)		Partial correlation coefficient (pH controlled)		Pearson correlation coefficient (SOC uncontrolled)		Partial correlation coefficient (SOC controlled)	
	20 cm	80 cm	20 cm	80 cm	20 cm	80 cm	20 cm	80 cm
$CaCl_2$-Si	0.708**	0.791**	0.656*	0.624*	–0.497	–0.650*	0.376	0.238
Acetic-Si	0.148	–0.137	0.441	0.470	0.069	0.362	0.424	0.557
H_2O_2-Si	0.919**	0.911**	0.849**	0.642*	–0.733**	–0.847**	0.410	–0.143
Oxalate-Si	–0.177	–0.185	0.480	0.404	0.433	0.384	0.596	0.511
Na_2CO_3-Si	0.957**	0.833**	0.831**	0.505	–0.855**	–0.769**	–0.089	–0.076

** Correlation is significant at $p < 0.01$; * Correlation is significant at $p < 0.05$

applied phytolith-rich straw (Table 1). Therefore, these correlations indicated that the application of phytolith-rich straw can result in the variation in the labile Si fractions by promoting the accumulation of soil organic matter, thus upon mineralization releasing phytoliths.

This study has found that the total labile Si content, irrespective of the groundwater level, significantly increased with increasing straw application (Table 2). However, this increase was driven by changes in the Na_2CO_3-Si and H_2O_2-Si contents (Table 2). In general, the dissolved Si in soil solution could be influenced by the interaction among different labile Si pools (Seyfferth

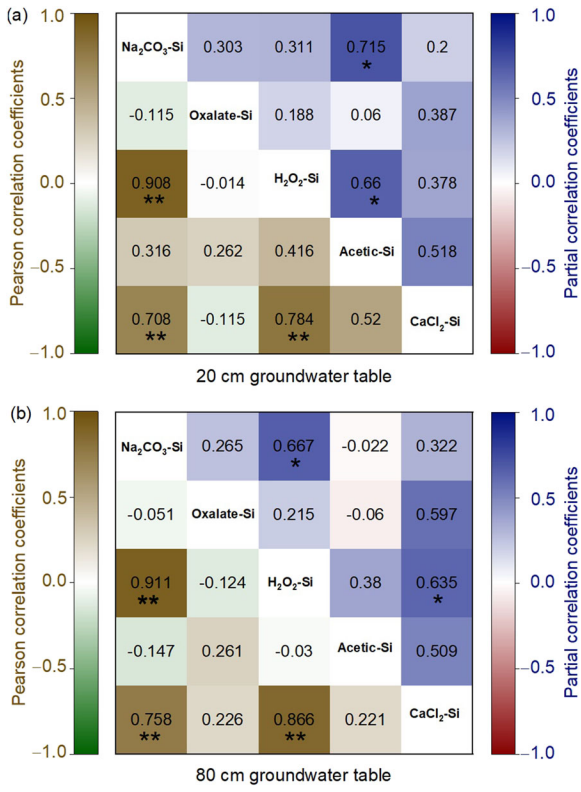

Fig. 3 Pearson correlation coefficients and partial correlation coefficients among the various labile Si fractions under 20 cm (**a**) and 80 cm (**b**) groundwater tables. ** Correlation is significant at $p < 0.01$; * Correlation is significant at $p < 0.05$

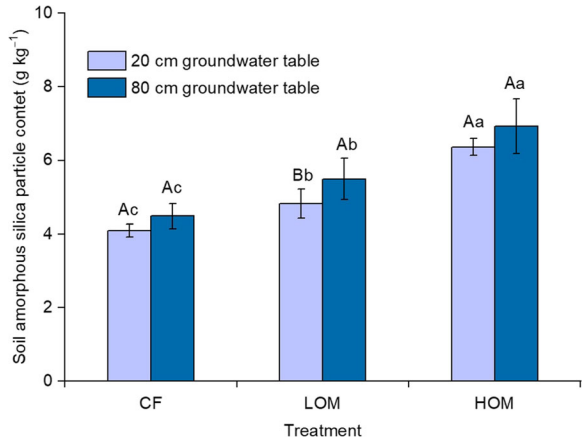

Fig. 4 Content of soil amorphous silica particles extracted by heavy liquid ($ZnBr_2$, $\rho = 2.3$ g cm^{-3}) suspension under the two groundwater tables. Different lower-case letters indicate significant differences among treatments under the same groundwater table at $p < 0.05$, based on the least significant difference (LSD) test. Different upper-case letters indicate significant differences of the same treatment under different groundwater tables at $p < 0.05$, based on the independent sample *t*-test. The error bars represent the standard deviation

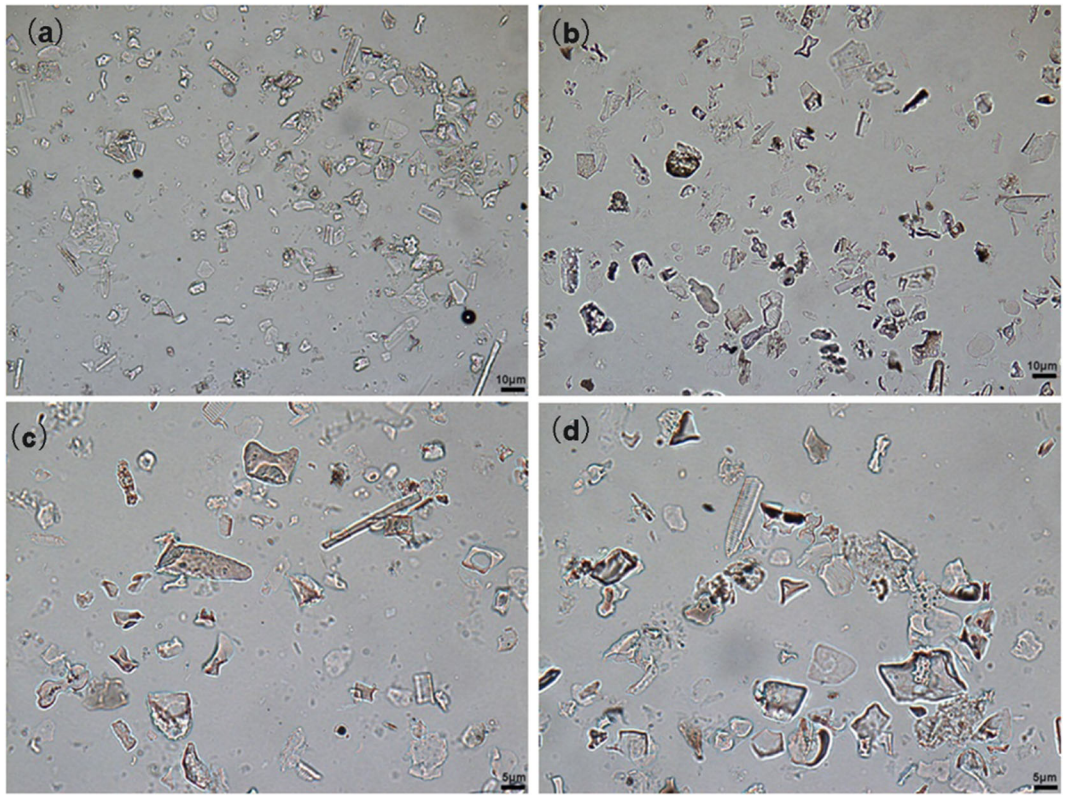

Fig. 5 Microphotographs with 200× (**a, b**) and 400× (**c, d**) magnification of soil amorphous particles extracted by heavy liquid ($ZnBr_2$, ρ = 2.3 g cm^{-3})

et al. 2013; Klotzbücher et al. 2015; Cornelis and Delvaux, 2016). As one of the major components of Na_2CO_3-Si (Cornelis et al. 2011), phytoliths can be released into soil when applied crop straw is degraded or mineralized. This is supported by the findings that the contents of amorphous silica particles mainly composed of phytoliths increased significantly with increasing straw application under both groundwater tables (Figs. 4 and 5). Our results showed that Na_2CO_3-Si made the biggest contribution to the labile Si pool (Table 2), which is consistent with previous studies (e.g., Saccone et al. 2007; Clymans et al. 2011; Cornelis et al. 2011; Klotzbücher et al. 2015). Because phytoliths are the largest component of the Na_2CO_3-Si pool (Fig. 5), their dissolution can lead to changes in other labile Si fractions. For example, recent studies implied that soil organic matter could loosely adsorb silicic acid on its surface (i.e., H_2O_2-Si) (Georgiadis et al. 2013, 2017; Song et al. 2014a; Liang et al. 2015; Yang et al. 2020). The significant partial correlation between SOC content and H_2O_2-Si content (Table 3) suggested that the accumulation of soil organic matter may offer more attachment points for the adsorption of silicic acid, thus effectively lowering leaching losses of Si.

A straw decomposition experiment conducted by Marxen et al. (2016) has shown that the loss of Si from straw occurred mainly during the first 33 days of incubation. Guo et al. (2015) reported that the Si content was significantly positively correlated with phytolith content in rice plant tissues (sheath, leaf, flag leaf, and stem). This means that the Si in rice straw was mainly deposited in the form of phytoliths. Therefore, the loss of Si from rice straw reported by Marxen et al. (2016) occurred mainly because of dissolution of straw phytoliths. Fraysse et al. (2010) also suggested that plant phytoliths govern the release of Si from plant material. It has been reported that the phytolith dissolution rate strongly depends on soil pH (Fraysse et al. 2006; Li et al. 2019). In this study, we found that the content of $CaCl_2$-Si, including mainly monosilicic acid and polysilicic acid (Cornelis et al. 2011), did not increase significantly upon application of phytolith-rich straw (Table 2). Previous studies reported that $CaCl_2$-Si

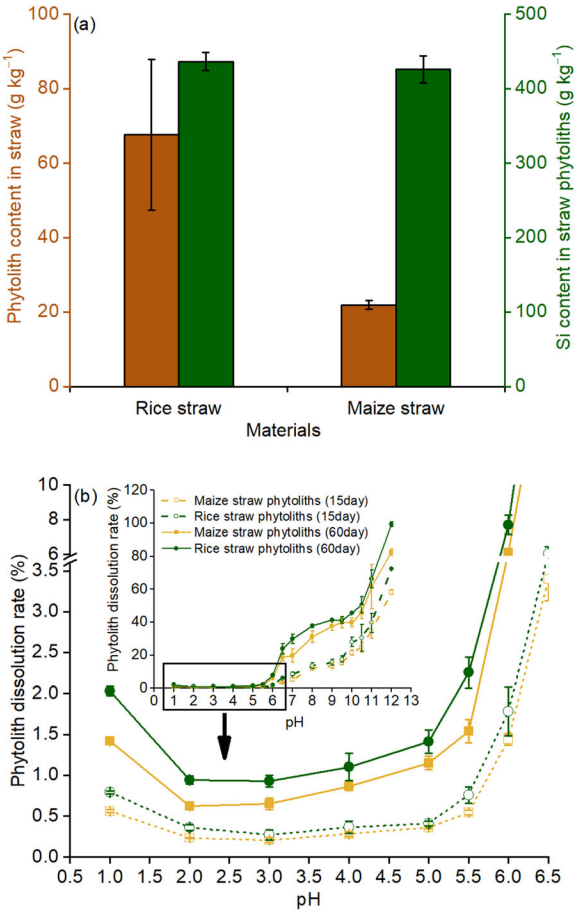

Fig. 6 Content of phytoliths extracted from supplied straw materials as well as the Si content in these phytoliths (a) and dissolution rate of these phytoliths under increasing pH (b). The error bars represent the standard deviation

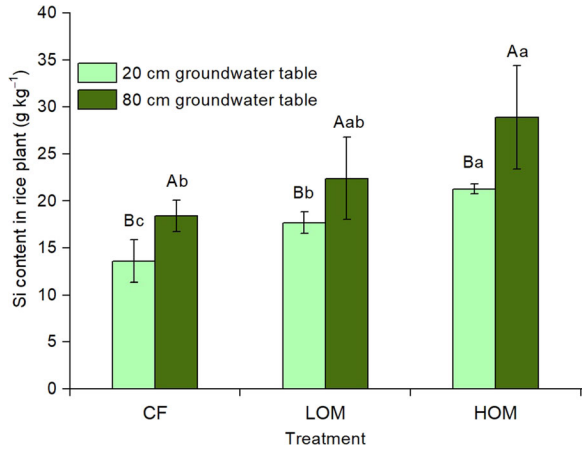

Fig. 7 Si content in planted rice straw under the two groundwater tables. Different lower-case letters indicate significant differences among treatments under the same groundwater table at $p < 0.05$, based on the least significant difference (LSD) test. Different upper-case letters indicate significant differences of the same treatment under different groundwater tables at $p < 0.05$, based on the independent sample *t*-test. The error bars represent the standard deviation

depends on soil pH, clay minerals, and may not be impacted by phytoliths (Miles et al. 2014; Meunier et al., 2018). However, in this study, the partial correlation analysis showed that $CaCl_2$-Si under the two groundwater tables were non-significantly correlated with soil pH (Table 3). Therefore, we assumed that the minor influence of soil pH on $CaCl_2$-Si was mainly due to the initial low soil pH and the low variation in range of soil pH (Table 1). To demonstrate the assumption, this study explored changes in the dissolution rates of phytoliths extracted from straws typically applied over the 36-year field trial. We found that the phytolith dissolution was relatively small after both 15 and 60 days of incubation where the solution pH ranging from 2 to 5.5 (Fig. 6b). The pH in the studied soils varied from 4.84 ± 0.02 to 5.45 ± 0.13 (Table 2), supporting the slow dissolution of phytoliths observed in the current study. Furthermore, phytoliths in natural soils are more stable than in tested solution due to the protection offered by soil microaggregates (Li et al. 2020b) and their interaction with soil iron or aluminum oxides and hydroxides (Cabanes et al. 2011; Song et al. 2018). Therefore, our results suggest that the pH had relatively little influence on the labile Si pools in acidic soils (pH < 5.5).

The Si content in the planted rice straw near harvest increased significantly with increasing straw application doses (Fig. 7). It can therefore be suggested that this could lower plant available Si content in soil (Seyfferth et al. 2013; Klotzbücher et al. 2015; Riotte el al. 2018), explaining the lack of response of soil $CaCl_2$-Si content to increasing straw addition (Table 2). In addition, as the only fraction that can be directly absorbed by the plant, dissolved Si is at the center of the interconversions among the various labile Si fractions (Cornelis and Delvaux 2016; Li and Delvaux 2019; Yang et al. 2020). Therefore, the uptake of dissolved Si by plants can promote the hydrolyzation, desorption, and dissolution of Si from different labile Si pools (Cornelis et al. 2011; White et al. 2012; Seyfferth et al. 2013; Klotzbücher et al. 2015; Cornelis and Delvaux 2016), while slow weathering of soil minerals can also release some monosilicic acid (Sommer et al. 2006; Cornelis and Delvaux 2016). It should also be noted that crop growth can influence Si release by accelerating the

weathering of straw phytoliths and soil minerals (Marxen et al. 2016; Li et al., 2020b). An important mechanism of the silicate weathering driven by plants is the rapid uptake of base cations and Si during plant growth (Balogh-Brunstad et al. 2008; Street-Perrott and Barker 2008; Uhlig et al. 2017). Another major mechanism is the changes in soil physical properties, particularly the exposed surface areas of minerals and the residence time of water, caused by plant roots (Drever 1994). As discussed above, because phytolith dissolution rates are fairly slow under acidic conditions (pH < 5.5), the increasing phytolith content caused by the direct return of phytolith-rich straw plays an important role in the long-term supply of bioavailable Si in paddy fields.

Effect of the groundwater table on the soil-plant Si cycle

It is well known that water percolation is a key driving factor for downward transport of soil particles and that this can be influenced by the groundwater table (Phillips 2007). Because soil phytoliths are an important component of soil particles, vertical migration of soil phytoliths can also be promoted by water percolation (Fishkis et al. 2009, 2010a). In this study, partial correlation analysis revealed that Na_2CO_3-Si content was significantly correlated to SOC under the 20 cm groundwater table, whereas there were no statistical dependencies under the 80 cm groundwater table (Table 3). The difference is likely due to the different vertical migration patterns of soil phytoliths resulting from different groundwater depths. This could be supported by the experiments on phytolith transport in sandy sediment (Fishkis et al. 2009) where greater irrigation (80 mm × 2 times per month) resulted in leaching of 22% of the applied phytoliths, while lower irrigation (40 mm × 2 times per month) leached 17%. In addition, the downward migration of phytoliths in soil can be affected by their size and shape (Fishkis et al. 2010a, b). Generally, small-sized phytoliths (circle-equivalent diameter < 5 μm) are most likely to be transported due to their greater probability of passing narrow pore channels, compared with larger phytoliths (circle-equivalent diameter > 5 μm) (Fishkis et al. 2010a). As the size and morphology of phytoliths were not determined in our study, the effects of phytolith size and shape on their downward migration under the two groundwater tables need further evaluation.

The multiple transformations among the labile Si fractions are an important process in the soil-plant Si cycle (Georgiadis et al. 2017; Li and Delvaux 2019; Yang et al. 2020). Generally, the intensity of redox reactions is closely related to changes in the groundwater table, which in turn can drive transformation processes among the various labile Si fractions (Saccone et al. 2008; Mihara et al. 2016; Siipola et al. 2016; Georgiadis et al. 2017). In this study, partial correlation analysis showed that the correlations among the various labile Si fractions under the 20 cm groundwater table were different from those under 80 cm groundwater table (Fig. 3). This means that the multiple transformation processes among the various labile Si fractions can be influenced by the groundwater table.

The $CaCl_2$-Si fraction is generally used to assess the changes in bioavailability of soil Si (e.g., Seyfferth et al. 2013; Miles et al. 2014; Meunier et al., 2018; Riotte el al. 2018). Our results showed that the $CaCl_2$-Si content under the 20 cm groundwater table was significantly lower than under the 80 cm groundwater table for both straw return rates (Table 2). This was likely caused by the stronger eluviation of plant-available Si under the 20 cm groundwater table. The 80 cm groundwater table could be regarded as one of water-saving irrigation practice in the region where the study was undertaken. Therefore, our results suggest that this water-saving irrigation practice can help to maintain or improve the bioavailability of soil Si in paddy field. This was further supported by the findings that the Si content in planted rice straw under the 80 cm groundwater table was significantly higher than under the 20 cm groundwater table for each treatment (Fig. 7).

Implications for sustainable agricultural development

In China, rice self-sufficiency has been achieved in recent years (CFNDC 2019; Deng et al. 2019). However, the rice consumption rate is increasing with the rise in population. Therefore, a challenge exists to increase rice yield, but on the limited area of paddy fields that will be available. It has been previously reported that Si deficiency in paddy fields is a key factor restricting sustainable development of rice production (Seyfferth et al. 2013; Song et al. 2014a; Liang et al. 2015; Marxen et al. 2016). In subtropical China, most paddy soils are acidic (Guo et al. 2010), and therefore, the dissolution rates of phytoliths in the studied soil (pH < 5.5) were low (Fig. 6). This low dissolution rate could, however, be balanced by a continuing supply of phytolith-rich crop straw to ensure adequate Si uptake. Therefore, the

phytolith-rich crop straw should be considered as an ideal Si fertilizer to supply bioavailable Si to soils over the long term and further increase the productivity of Si-accumulating plants. Furthermore, for the same phytolith-rich straw application, the Si contents in planted rice straw under the 80 cm groundwater table were significantly higher than under the 20 cm groundwater table (Fig. 7). This suggests that groundwater table management, and in particular, water saving irrigation practices, play an important role in regulating the soil bioavailable Si supply in paddy fields.

Conclusions

Our results showed that the total labile Si content increased significantly with increasing phytolith-rich straw application. Within the labile Si fractions, the largest fraction was Na_2CO_3-Si, followed by Oxalate-Si, H_2O_2-Si, Acetic-Si, and $CaCl_2$-Si. Among these subfractions, the contents of Na_2CO_3-Si and H_2O_2-Si increased significantly with increasing phytolith-rich straw application, explaining the increases in labile Si content. As one of indicators of plant-available Si in soil, the $CaCl_2$-Si content did not show significant differences among different treatments. However, the Si content in the planted rice straw increased significantly with increasing phytolith-rich straw application. These findings indicate that long-term application of phytolith-rich straw is beneficial for providing adequate Si for rice production and enhancing the soil-plant Si cycle.

The $CaCl_2$-Si content under the 80 cm groundwater table was greater than that under the 20 cm groundwater table for the same application dose of phytolith-rich straw. Correspondingly, the Si contents in planted rice straw under the 80 cm groundwater table were significantly higher than under the 20 cm groundwater table for the same phytolith-rich straw application. These findings imply that soil Si bioavailability as well as soil-plant Si cycle are affected by the height of the groundwater table.

The present study suggests that long-term application of phytolith-rich straw and the maintenance of the groundwater table significantly influence the soil-plant Si cycle and further increase soil Si bioavailability by promoting the accumulations of soil organic matter and soil phytoliths. Therefore, returning phytolith-rich straw in conjunction with the groundwater table management should be considered as feasible and useful long-term practice to regulate the supply of bioavailable Si in paddy fields.

Acknowledgements We acknowledge the support from the National Natural Science Foundation of China (41930862, 41522207 and 41571130042) and the State's Key Project of Research and Development Plan of China (2016YFA0601002 and 2017YFC0212703).

Compliance with ethical standards

Conflict of interest The authors declare no conflict of interests.

References

Balogh-Brunstad Z, Keller CK, Bormann BT, O'Brien R, Wang D, Hawley G (2008) Chemical weathering and chemical denudation dynamics through ecosystem development and disturbance. Glob Biogeochem Cycles 22:GB1007

Barão L, Clymans W, Vandevenne F, Meire P, Conley DJ, Struyf E (2014) Pedogenic and biogenic alkaline-extracted silicon distributions along a temperate land-use gradient. Eur J Soil Sci 65:693–705

Beardmore J, Lopez X, Mujika JI, Exley C (2016) What is the mechanism of formation of hydroxyaluminosilicates? Sci Rep 6:8

Cabanes D, Weiner S, Shahack-Gross R (2011) Stability of phytoliths in the archaeological record: a dissolution study of modern and fossil phytoliths. J Archaeol Sci 38(9):2480–2490

Cao Y, Wang J, Huang H, Sun E, Butterly C, Xu Y, He H, Zhang J, Chang Z (2019) Spectroscopic evidence for hyperthermophilic pretreatment intensifying humification during pig manure and rice straw composting. Bioresource Technol 294:122131

China Food Network Data Center (CFNDC) (2019) http://datacenter.cngrain.com

Clymans W, Struyf E, Govers G, Vandevenne F, Conley DJ (2011) Anthropogenic impact on amorphous silica pools in temperate soils. Biogeosciences 8:2281–2293

Cornelis JT, Delvaux B (2016) Soil processes drive the biological silicon feedback loop. Func Ecol 30:1298–1310

Cornelis JT, Titeux H, Ranger J, Delvaux B (2011) Identification and distribution of the readily soluble silicon pool in a temperate forest soil below three distinct tree species. Plant Soil 342:369–378

Coskun D, Deshmukh R, Sonah H, Menzies JG, Reynolds O, Ma JF, Kronzucker HJ, Bélanger RR (2019) The controversies of silicon's role in plant biology. New Phytol 221(1):67–85

DeMaster DJ (1981) The supply and accumulation of silica in the marine environments. Geochim Cosmochim Acta 45:1715–1732

Deng N, Grassini P, Yang H, Huang J, Cassman KG, Peng S (2019) Closing yield gaps for rice self-sufficiency in China. Nat Commun 10(1):1725

Dobermann A, Fairhurst TH (2002) Rice straw management. Better Crop Int 16(1):7–11

Domínguez-Escribá L, Porcar M (2010) Rice straw management: the big waste. Biofuels Bioprod Bior 4(2):154–159

Drever JI (1994) The effect of land plants on the weathering rates of silicate minerals. Geochim Cosmochim Acta 58:2325–2332

Epstein E (1999) Silicon. Annu Rev Plant Physio 50:641–664

Fishkis O, Ingwersen J, Streck T (2009) Phytolith transport in sandy sediment: experiments and modeling. Geoderma 151: 168–178

Fishkis O, Ingwersen J, Lamers M, Denysenko D, Streck T (2010a) Phytolith transport in soil: a laboratory study on intact soil cores. Eur J Soil Sci 61(4):445–455

Fishkis O, Ingwersen J, Lamers M, Denysenko D, Streck T (2010b) Phytolith transport in soil: a field study using fluorescent labelling. Geoderma 157:27–36

Fraysse F, Pokrovsky OS, Schott J, Meunier JD (2006) Surface properties, solubility and dissolution kinetics of bamboo phytoliths. Geochim Cosmochim Acta 70:1939–1951

Fraysse F, Pokrovsky OS, Schott J, Meunier JD (2009) Surface chemistry and reactivity of plant phytoliths in aqueous solutions. Chem Geol 258:197–206

Fraysse F, Pokrovsky OS, Meunier JD (2010) Experimental study of terrestrial plant litter interaction with aqueous solutions. Geochim Cosmochim Acta 74:70–84

Georgiadis A, Sauer D, Herrmann L, Breuer J, Zarei M, Stahr K (2013) Development of a method for sequential Si extraction from soils. Geoderma 209:251–261

Georgiadis A, Rinklebe J, Straubinger M, Rennert T (2017) Silicon fractionation in Mollic Fluvisols along the Central Elbe River, Germany. Catena 153:100–105

Gotoh S, Onikura Y (1971) Organic acids in a flooded soil receiving added rice straw and their effect on the growth of rice. Soil Sci Plant Nutr 17(1):1–8

Guntzer F, Keller C, Poulton P, McGrath S, Meunier JD (2012) Long-term removal of wheat straw decreases soil amorphous silica at Broadbalk, Rothamsted. Plant Soil 352:173–184

Guo J, Liu X, Zhang Y, Shen J, Han W, Zhang W, Christie P, Goulding KWT, Vitousek PM, Zhang F (2010) Significant acidification in major Chinese croplands. Science 327(5968): 1008–1010

Guo F, Song Z, Sullivan L, Wang H, Liu X, Wang X, Li Z, Zhao Y (2015) Enhancing phytolith carbon sequestration in rice ecosystems through basalt powder amendment. Sci Bull 60:591–597

Haysom MBC, Chapman LS (1975) Some aspects of the calcium silicate trials at Mackay. Proc Qld Soc Sugar Cane Technol 42:117–122

Hodson MJ, Sangster AG (1999) Aluminium/silicon interactions in conifers. J Inorg Biochem 76:89–98

IUSS Working Group WRB (2015) World reference base for soil resources 2014, Update 2015, International soil classification system for naming soils and creating legends for soil maps. World Soil Resources Reports No. 106. FAO, Rome

Jones LHP, Handreck KA (1963) Effects of iron and aluminium oxides on silica in solution in soils. Nature 198:852–853

Jones DL, Dennis PG, Owen AG, van Hees PAW (2003) Organic acids behavior in soils-misconceptions and knowledge gaps. Plant Soil 248:31–41

Keller C, Guntzer F, Barboni D, Labreuche J, Meunier J-D (2012) Impact of agriculture on the Si biogeochemical cycle: input from phytolith studies. Compt Rendus Geosci 344:739–746

Klotzbücher T, Leuther F, Marxen A, Vetterlein D, Horgan FG, Jahn R (2015) Forms and fluxes of potential plant-available silicon in irrigated lowland rice production (Laguna, the Philippines). Plant Soil 393:177–191

Klotzbücher A, Klotzbücher T, Jahn R, Van Chien H, Hinrichs M, Sann C, Vetterlein D (2018) Effects of Si fertilization on Si in soil solution, Si uptake by rice, and resistance of rice to biotic stresses in Southern Vietnam. Paddy Water Environ 16(2): 243–252

Li Z, Delvaux B (2019) Phytolith-rich biochar: A potential Si fertilizer in desilicated soils. GCB Bioenergy 11:1264–1283

Li Z, Song Z, Parr JF, Wang H (2013) Occluded C in rice phytoliths: implications to biogeochemical carbon sequestration. Plant Soil 370:615–623

Li Z, Unzué-Belmonte D, Cornelis JT, Vander Linden C, Struyf E, Ronsse F, Delvaux B (2019) Effects of phytolithic rice-straw biochar, soil buffering capacity and pH on silicon bioavailability. Plant Soil 438:187–203

Li Z, Cornelis JT, Linden CV, Van Ranst E, Delvaux B (2020a) Neoformed aluminosilicate and phytogenic silica are competitive sinks in the silicon soil–plant cycle. Geoderma 368: 114308

Li Z, de Tombeur F, Vander Linden C, Cornelis JT, Delvaux B (2020b) Soil microaggregates store phytoliths in a sandy loam. Geoderma 360:114037

Liang Y, Nikolic M, Bélanger R, Gong H, Song A (2015) Silicon in agriculture. From theory to practice. Springer, Dordrecht

Lin Q, Liao C, Dai Q, Tang R, Sun Y, Xie L, Li L (2018) Effect of long-term fertilization and groundwater level on microaggregate distribution and its fractal feature in red paddy soil. Chinese J Soil Sci 49:1397–1404 (in Chinese with English abstract)

Lu R (2000) Methods of soil and agrochemical analysis. China Agricultural Science and Technology Press, Beijing (in Chinese)

Ma JF, Yamaji N (2006) Silicon uptake and accumulation in higher plants. Trends Plant Sci 11(8):392–397

Marxen A, Klotzbücher T, Jahn R, Kaiser K, Nguyen VS, Schmidt A, Schädler M, Vetterlein D (2016) Interaction between silicon cycling and straw decomposition in a silicon deficient rice production system. Plant Soil 398:153–163

Memon M, Guo J, Tagar A, Perveen N, Ji C, Memon S, Memon N (2018) The effects of tillage and straw incorporation on soil organic carbon status, rice crop productivity, and sustainability in the rice-wheat cropping system of eastern China. Sustainability 10(4):961

Meunier JD, Keller C, Guntzer F, Riotte J, Braun JJ, Anupama K (2014) Assessment of the 1% Na_2CO_3 technique to quantify the phytolith pool. Geoderma 216:30–35

Meunier JD, Sandhya K, Prakash NB, Borschneck D, Dussouillez P (2018) pH as a proxy for estimating plant-available Si? A case study in rice fields in Karnataka (South India). Plant Soil 432(1–2):143–155

Mihara C, Makabe-Sasaki S, Watanabe A (2016) Dynamics of dissolved silicon in rice paddies under conditions of water conservation irrigation. J Soil Sediment 16(2):547–556

Miles N, Manson AD, Rhodes R, Van Antwerpen R, Weigel A (2014) Extractable silicon in soils of the south African

industry and relationships with crop uptake. Commun Soil Sci Plant Anal 45:2949–2958

Parr JF, Sullivan LA (2014) Comparison of two methods for the isolation of phytolith occluded carbon from plant material. Plant Soil 374:45–53

Phillips JD (2007) Development of texture contrast soils by a combination of bioturbation and translocation. Catena 70(1):92–104

Pokrovski GS, Schott J, Farges F, Hazemann JL (2003) Iron (III)-silica interactions in aqueous solution: insights from X-ray absorption fine structure spectroscopy. Geochim Cosmochim Ac 67:3559–3573

Riotte J, Sandhya K, Prakash NB, Audry S, Zambardi T, Chmeleff J, Buvaneshwari S, Meunier JD (2018) Origin of silica in rice plants and contribution of diatom earth fertilization: insights from isotopic Si mass balance in a paddy field. Plant Soil 423:481–501

Saccone L, Conley DJ, Koning E, Sauer D, Sommer M, Kaczorek D, Blecker SW, Kelly EF (2007) Assessing the extraction and quantification of amorphous silica in soils of forest and grassland ecosystems. Eur J Soil Sci 58:1446–1459

Saccone L, Conley DJ, Likens GE, Bailey SW, Buso DC, Johnson CE (2008) Factors that control the range and variability of amorphous silica in soils in the Hubbard Brook Experimental Forest. Soil Sci Soc Am J 72:1637–1644

Sauer D, Saccone L, Conley DJ, Herrmann L, Sommer M (2006) Review of methodologies for extracting plant-available and amorphous Si from soils and aquatic sediments. Biogeochemistry 80:89–108

Seyfferth AL, Kocar BD, Lee JA, Fendorf S (2013) Seasonal dynamics of dissolved silicon in a rice cropping system after straw incorporation. Geochim Cosmochim Acta 123:120–133

Siipola V, Lehtimäki M, Tallberg P (2016) The effects of anoxia on Si dynamics in sediments. J Soil Sediment 16:266–279

Sommer M, Kaczorek D, Kuzyakov Y, Breuer J (2006) Silicon pools and fluxes in soils and landscapes –A review. J Plant Nutr Soil Sci 169:310–3291

Song Z, Wang H, Strong PJ, Shan S (2014a) Increase of available soil silicon by Si-rich manure for sustainable rice production. Agron Sustain Dev 34:813–819

Song Z, Wang H, Strong PJ, Guo F (2014b) Phytolith carbon sequestration in China's croplands. Eur J Agron 53:10–15

Song A, Ning D, Fan F, Li Z, Liang Y (2015) The potential for carbon bio-sequestration in china's paddy rice (*oryza sativa* L.) as impacted by slag-based silicate fertilizer. Sci Rep 5: 17354

Song Z, Liu C, Müller K, Yang X, Wu Y, Wang H (2018) Silicon regulation of soil organic carbon stabilization and its potential to mitigate climate change. Earth-Sci Rev 185:463–475

Street-Perrott FA, Barker PA (2008) Biogenic silica: a neglected component of the coupled global continental biogeochemical cycles of carbon and silicon. Earth Surf Process Landf 33: 1436–1457

Strobel BW (2001) Influence of vegetation on low-molecular weight carboxylic acids in soil solution–A review. Geoderma 99:169–198

Takahashi E, Ma JF, Miyake Y (1990) The possibility of silicon as an essential element for higher plants. Comments Agric Food Chem 2:99–102

Uhlig D, Schuessler JA, Bouchez J, Dixon JL, von Blanckenburg F (2017) Quantifying nutrient uptake as driver of rock weathering in forest ecosystems by magnesium stable isotopes. Biogeosciences 14(12):3111

Walkley A, Black IA (1934) An examination of the Degtjareff method for determining soil organic matter, and a proposed modification of the chromic acid titration method. Soil Sci 37:29–38

Wang H, Hijmans RJ (2019) Climate change and geographic shifts in rice production in China. Environ Res Commun 1:011008

White AF, Vivit DV, Schulz MS, Bullen TD, Evett RR, Aagarwal J (2012) Biogenic and pedogenic controls on Si distributions and cycling in grasslands of the Santa Cruz soil chronosequence, California. Geochim Cosmochim Acta 94: 72–94

Yang X, Song Z, Yu C, Ding F (2020) Quantification of different silicon fractions in broadleaf and conifer forests of northern China and consequent implications for biogeochemical Si cycling. Geoderma 361:114036

Yin L, Zhang L, Yi Y, Luo F (2015) Effects of long-term groundwater management and straw application on aggregation of paddy soils in subtropical China. Pedosphere 25:386–391

Zuo X, Lu H, Gu Z (2014) Distribution of soil phytolith-occluded carbon in the Chinese Loess Plateau and its implications for silica–carbon cycles. Plant Soil 374:223–232